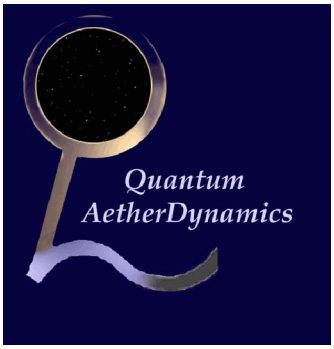

Quantum AetherDynamics Institute (QADI)

Rotational Propagation Geometry and the Origin of Gravitational Closure: A Loxodromic QMU Interpretation of Horizons, Clock-Rate Variation, and Phase Compression

David W. Thomson III
Quantum AetherDynamics Institute (QADI), Alma, Illinois, USA
ORCID: 0000-0002-5830-5427

Version 1.0 – May 17, 2026

This article is published by the Quantum AetherDynamics Institute (QADI).

It develops the Aether Physics Model (APM)

Abstract

Previous papers in the QMU Planck–Aether closure series demonstrated that the Planck system emerges from a bridge relation between the electron mass and the Aether maximum mass, and that the Aether maximum mass corresponds to the Schwarzschild closure condition:

$$\frac{Gm_a}{c^2} = \lambda_C.$$

The present paper develops the physical propagation geometry underlying this closure condition.

Within the Aether Physics Model (APM), propagation is interpreted as rotational and loxodromic rather than purely linear. Gravity is consequently reinterpreted as rotational phase compression within propagation geometry itself.

The Ledger One identity:

$$A_u \cdot \mathrm{curl} = {F_q}^2 {\lambda_C}^2 = c^2$$

is shown to define the maximum stable propagation condition of rotational space. Increasing gravitational concentration compresses available propagation-phase geometry, producing propagation delay, clock-rate variation, redshift, and horizon formation.

In this interpretation, black-hole horizons correspond to closure-locked propagation boundaries rather than coordinate singularities. The Planck scale becomes a crossover geometry between localized rotational closure and maximum propagation closure.

The framework additionally predicts natural ultraviolet propagation cutoffs, scalar gravitational-wave modes, rotational magnetometer effects, and closure-dependent phase phenomena accessible to experimental investigation.

Keywords: QMU, APM, loxodromic propagation, gravitational closure, chronovibration, Ledger One, black holes, clock-rate variation, scalar gravitational waves, rotational geometry

1 Introduction

The previous papers in the QMU Planck–Aether closure series established two central identities:

$$m_P^2 = \frac{m_e m_a}{2\pi}, \tag{1}$$

and:

$$\frac{Gm_a}{c^2} = \lambda_C. \tag{2}$$

These results demonstrated that the Planck system emerges from the span between localized electron closure and maximum gravitational propagation closure.

The present paper investigates the propagation geometry underlying these closure relations.

Within the Aether Physics Model (APM), propagation is not fundamentally linear. Instead, propagation occurs through rotational and loxodromic phase geometry associated with quantized Aether structure.

Gravity consequently emerges not as curvature acting on passive spacetime coordinates, but as compression of rotational propagation geometry itself.

This interpretation allows gravitational closure, black-hole horizons, propagation delay, and clock-rate variation to be treated as manifestations of a single underlying propagation mechanism.

2 Ledger One and Rotational Propagation

The primary propagation identity within QMU is:

$$c = \lambda_C F_q. \tag{3}$$

The corresponding propagation-square identity becomes:

$$c^2 = {\lambda_C}^2 {F_q}^2. \tag{4}$$

Within QMU, this relation corresponds directly to Ledger One:

$$A_u \cdot \mathrm{curl} = {F_q}^2 {\lambda_C}^2 = c^2. \tag{5}$$

This use of Ledger One follows the QMU foundational ledger convention developed in prior APM/QMU reference work Thomson [2025b,a]. This identity follows the QMU ledger convention in which A_u represents the rotational Aether unit and curl represents the torsional rotational-density operator; their product gives the propagation-square closure condition.

The quantity A_u represents rotational propagation structure, while curl represents rotational torsion density within the Aether ledger.

The product:

$$A_u \cdot \mathrm{curl} \tag{6}$$

therefore defines the maximum stable propagation condition of rotational geometry.

Within this framework, the speed of light is not merely a velocity parameter. It is the maximum stable rotational propagation rate permitted by Ledger One.

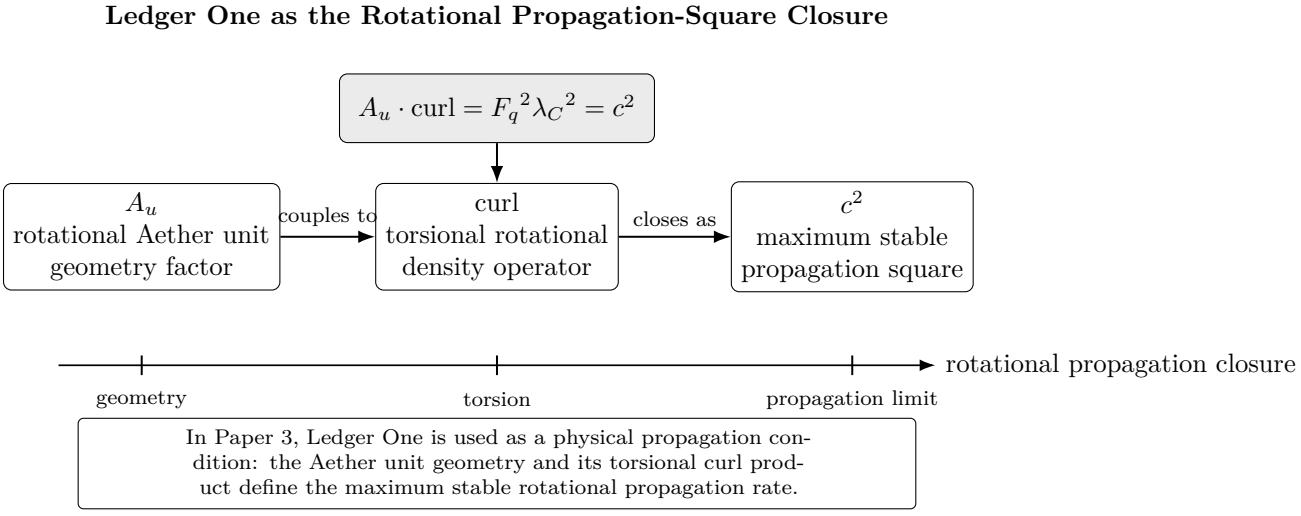

Figure 1: Ledger One interpreted as the propagation-square closure condition. The equation is not drawn as a decorative identity; it is the structural bridge between rotational Aether geometry, torsional density, and the observable propagation limit c^2.

3 Loxodromic Propagation Geometry

Within APM, propagation advances through continuous rotational spiral structure rather than through purely linear displacement.

This propagation geometry is loxodromic.

A loxodrome is a continuously advancing spiral path maintaining a fixed rotational angle while traversing curved geometry. Similar propagation structures appear naturally in rotating electromagnetic systems, helical waveguides, and holonomic transport systems Sagnac [1913], Aharonov and Bohm [1959], Berry [1984].

Within QMU, rotational propagation geometry produces continuous chronovibrational advancement through quantized propagation space.

The propagation state may therefore be interpreted as a continuously advancing rotational phase structure:

$$\Psi(s,t) \sim e^{i\theta(s,t)}, \tag{7}$$

where θ represents the propagation-phase geometry along propagation coordinate s.

Clock rates consequently emerge from propagation-phase advancement rates rather than from movement among separate time frames.

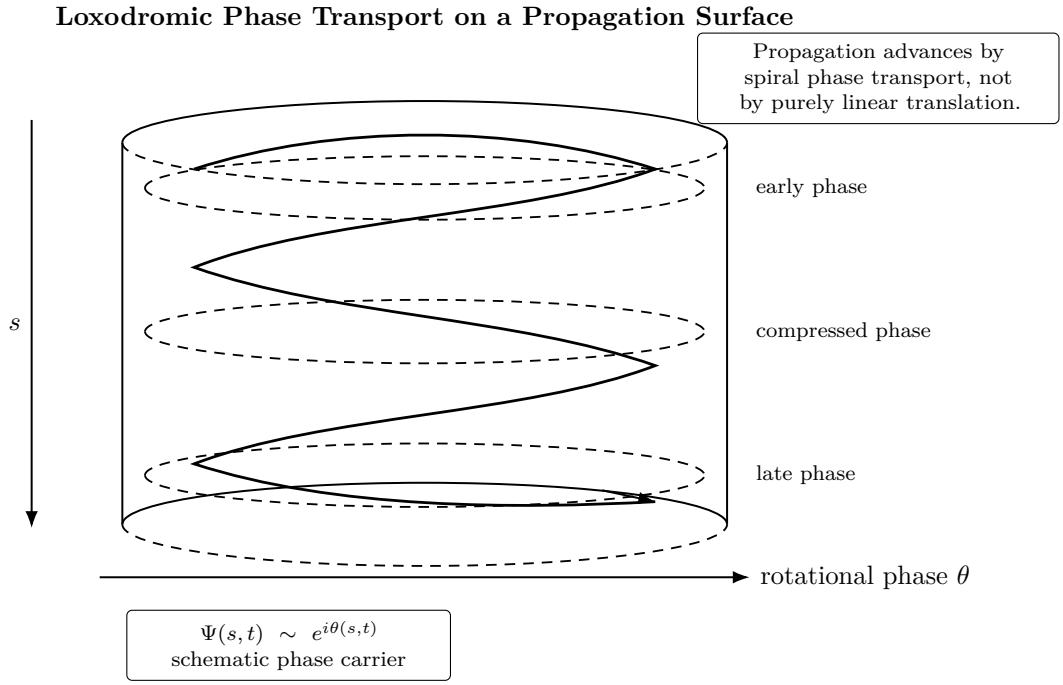

Figure 2: Loxodromic propagation represented as spiral phase transport on a propagation surface. The diagram emphasizes phase advancement along a propagation coordinate s while retaining rotational phase θ.

4 Rotational Phase Compression

The central proposition of the present paper is that gravity corresponds to rotational phase compression.

As gravitational loading increases, available propagation geometry becomes compressed.

The local propagation phase density may be expressed schematically as:

$$\Phi_g \sim \frac{\partial \theta}{\partial s}, \tag{8}$$

where increasing gravitational loading corresponds to increasing rotational phase density. This expression is schematic and is used only to identify the propagation phase variable; it is not intended as a complete wave-equation derivation.

As propagation geometry compresses:

- propagation path length increases,
- outward propagation freedom decreases,
- phase advancement slows,
- and local clock rates decrease.

This interpretation differs fundamentally from models involving movement between time frames.

Within APM, clock-rate variation occurs entirely within the continuously advancing present moment.

The experimentally observed gravitational redshift and clock-rate variations Pound and Rebka [1960], Hafele and Keating [1972b,a], Ashby [2003] therefore correspond to propagation-rate changes arising from compressed rotational geometry.

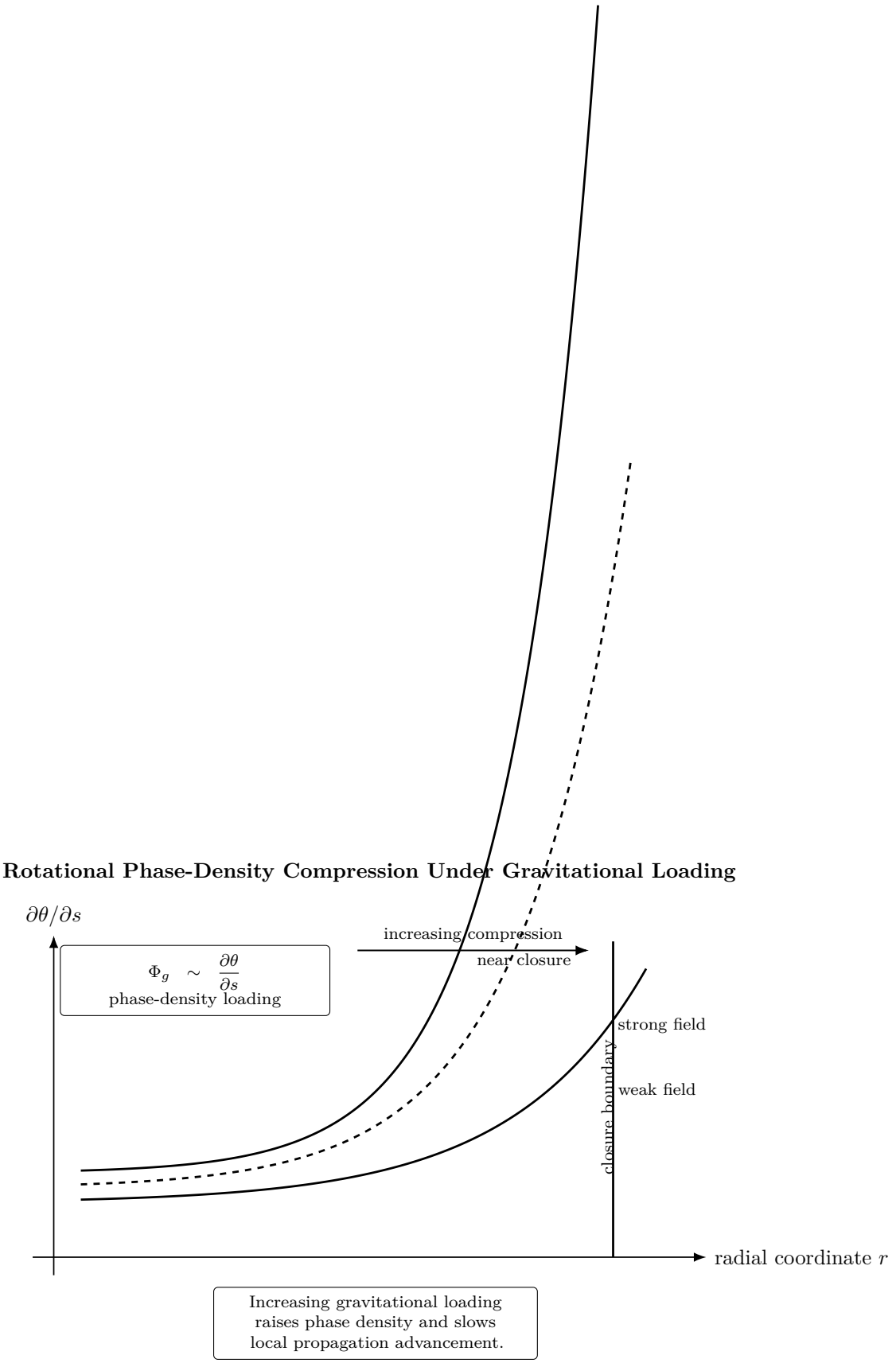

Figure 3: Schematic phase-density compression. Gravity is represented as increasing rotational phase density $\partial\theta/\partial s$, producing propagation delay and reduced local clock rate within the present moment.

5 Clock-Rate Variation and Gravitational Redshift

In general relativity, gravitational time dilation is typically described geometrically through metric curvature Einstein [1916], Wald [1984].

Within QMU, the same observational effects are reinterpreted as propagation-phase slowdown.

Increasing gravitational loading reduces local propagation advancement rates:

$$F_q{}' < F_q. \tag{9}$$

Since clock rates emerge from propagation advancement frequencies, local clocks advance more slowly under increased propagation compression.

Gravitational redshift consequently becomes a direct manifestation of reduced propagation-phase advancement.

This interpretation preserves experimentally verified clock-rate observations while providing a physical propagation mechanism beneath the metric description.

Clock-Rate Variation as Propagation-Frequency Change

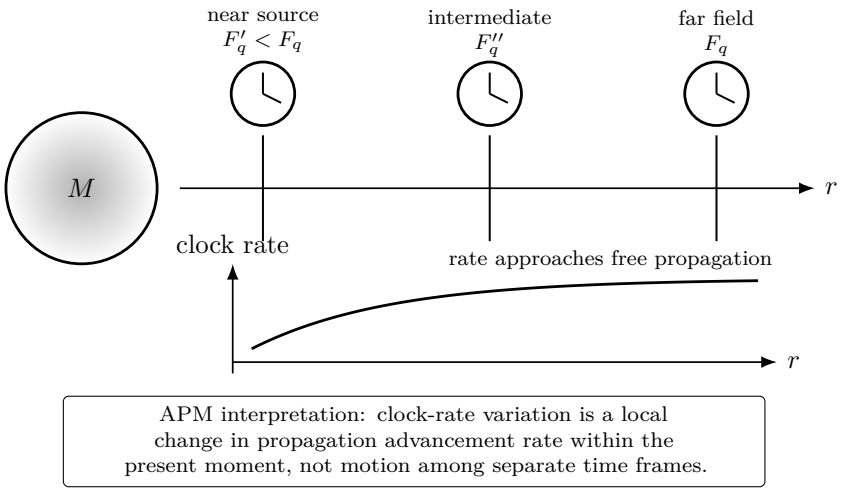

Figure 4: Clock-rate variation represented as a local change in propagation frequency. The diagram avoids time-frame language and treats gravitational redshift as a clock-rate effect caused by propagation compression.

6 Schwarzschild Closure and Horizon Formation

The Schwarzschild closure condition is:

$$r_s = \frac{Gm}{c^2}. \tag{10}$$

The previous paper demonstrated that:

$$\frac{Gm_a}{c^2} = \lambda_C. \tag{11}$$

This identity implies that gravitational closure occurs when rotational propagation compresses to the Compton propagation boundary.

Within this framework:

- weak gravitational fields correspond to mild propagation compression,
- strong gravitational fields correspond to severe propagation compression,
- and Schwarzschild closure corresponds to complete outward propagation trapping.

The black-hole horizon therefore becomes:

> A closure-locked propagation boundary where outward chronovibrational transport collapses.

This interpretation avoids treating singularities as physically infinite objects.

Instead, singularities arise from extending SI continuum projections beyond the physically permitted rotational propagation boundary.

Horizon Formation as Closure-Locked Propagation Boundary

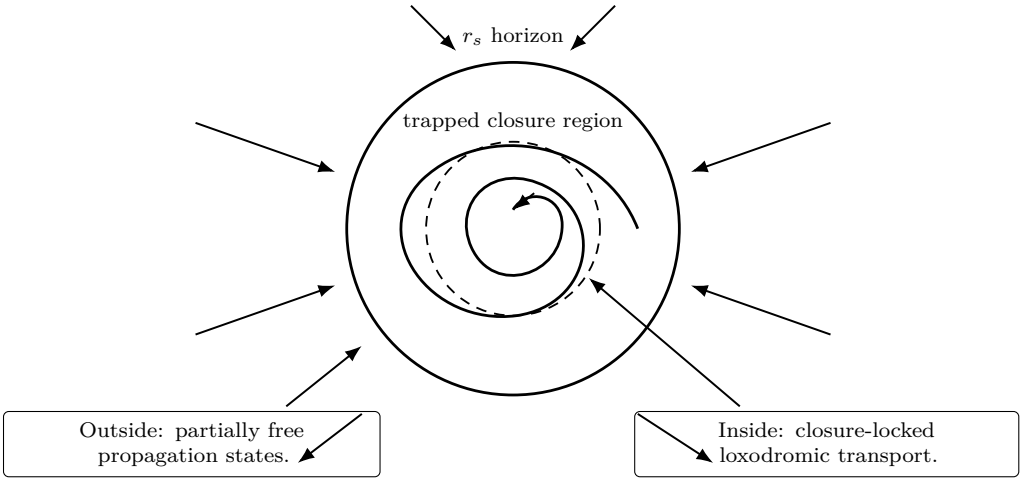

Figure 5: Horizon formation as a closure-locked propagation boundary. Outward propagation remains partially free outside the horizon but becomes trapped as loxodromic transport inside the closure surface.

7 Black-Hole Interior Geometry

The Kerr rotational solutions Kerr [1963] become especially important within the rotational propagation framework.

Because propagation itself is rotational, rotating black holes naturally preserve partial propagation ordering within closure geometry.

The black-hole interior may therefore be interpreted as:

- trapped loxodromic propagation states,
- closure-locked rotational transport,
- and chronovibrational phase compression.

The horizon surface becomes a propagation-boundary transition layer separating partially free propagation from fully trapped propagation geometry.

Black-hole thermodynamic relations Bardeen et al. [1973], Bekenstein [1973], Hawking [1975] may consequently emerge from closure-surface propagation degrees of freedom rather than from purely statistical coordinate arguments.

8 Scalar and Longitudinal Propagation Modes

The rotational propagation framework naturally permits scalar and longitudinal gravitational modes.

Within the QMU detector framework, scalar longitudinal propagation may be represented schematically as:

$$\mathrm{sclw}_d^* = \frac{1}{F_q}\partial_t \partial_x \xi, \tag{12}$$

where ξ represents propagation displacement within the rotational propagation medium. This detector expression is likewise schematic at this stage and serves as a compact representation of longitudinal propagation modulation in the RMFD detector framework.

Because gravity corresponds to rotational phase compression, propagating gravitational disturbances may produce measurable:

- phase delays,
- rotational magnetometer perturbations,
- longitudinal compression modes,
- and chronovibrational modulation signatures.

These effects provide possible observational pathways for testing the rotational propagation framework.

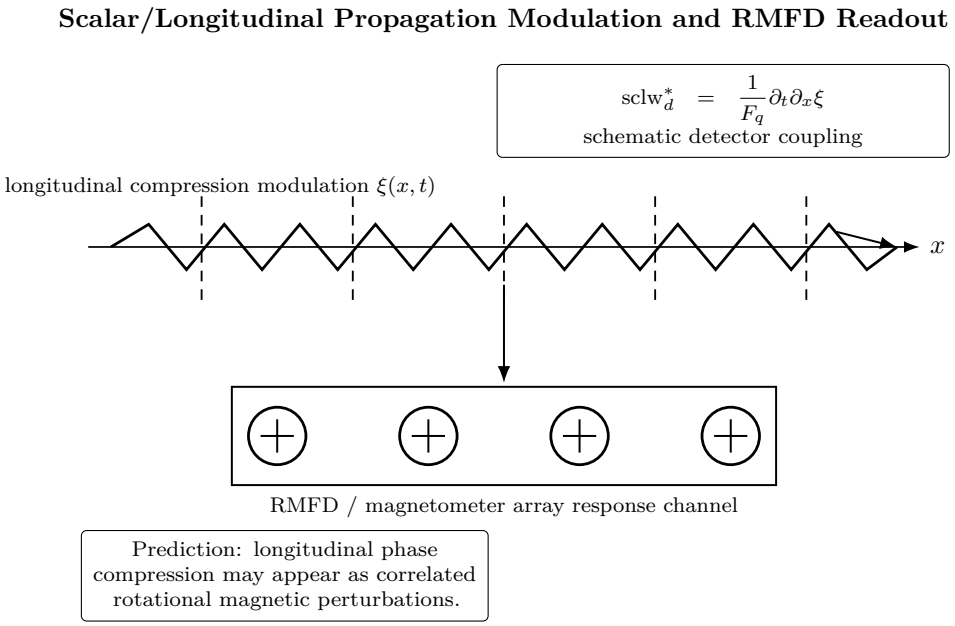

Figure 6: Schematic scalar/longitudinal propagation modulation coupled to an RMFD-style readout array. The expression is intentionally schematic and represents detector coupling rather than a complete field equation.

9 Natural Ultraviolet Closure Scale

The Schwarzschild–Compton closure identity:

$$\frac{Gm_a}{c^2} = \lambda_C \tag{13}$$

implies a natural ultraviolet propagation boundary associated with Compton-scale closure geometry.

In this interpretation, ultraviolet divergences arise when continuum coordinate models are extended beyond physically permitted rotational propagation structure.

The closure condition therefore suggests a natural geometric regularization mechanism for ultraviolet divergences in quantum-gravitational systems.

10 Experimental and Observational Predictions

The rotational propagation framework produces several potentially testable predictions.

10.1 Clock-Rate Variation

Gravitational clock-rate changes correspond to local propagation-rate variation rather than movement among time frames.

10.2 Scalar Gravitational Modes

Longitudinal and scalar gravitational-wave signatures may appear within RMFD-based magnetometer systems.

10.3 Rotational Magnetometer Effects

Rotational propagation compression may produce weak correlated magnetic perturbations near strong propagation-gradient systems.

10.4 Closure Harmonics

Black-hole closure boundaries may exhibit quantized rotational harmonic structures associated with trapped propagation states.

10.5 Ultraviolet Closure Boundary

Propagation geometry should exhibit natural closure cutoffs near the Compton propagation boundary.

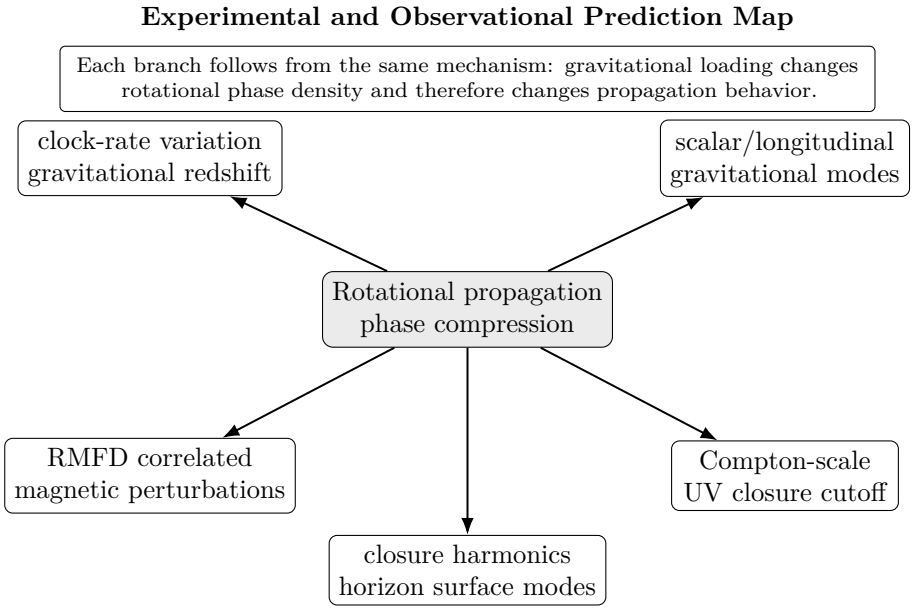

Figure 7: Prediction map for Paper 3. The diagram separates established clock-rate/redshift observables from proposed RMFD, scalar-mode, UV-closure, and horizon-harmonic tests.

11 Scientific Implications

The present analysis produces several important implications.

11.1 Gravity Becomes Propagation Compression

Gravity emerges from rotational phase compression within propagation geometry itself.

11.2 Clock Rates Become Propagation Rates

Observed gravitational clock-rate variation corresponds to altered propagation advancement rates within the present moment.

11.3 Horizons Become Propagation Boundaries

Black-hole horizons correspond to closure-locked propagation boundaries rather than infinitely dense singularities.

11.4 The Planck System Remains Emergent

The Planck scale remains a crossover layer between localized closure and maximum propagation closure.

11.5 Ledger One Unifies Propagation Physics

The Ledger One identity:

$$A_u \cdot \mathrm{curl} = c^2 \tag{14}$$

provides a unified rotational ledger connecting propagation geometry, electromagnetism, and gravitational closure.

12 Conclusion

The rotational propagation geometry underlying gravitational closure has been investigated within the Quantum Measurement Units framework of the Aether Physics Model.

The Ledger One identity:

$$A_u \cdot \mathrm{curl} = {F_q}^2 {\lambda_C}^2 = c^2 \tag{15}$$

defines the maximum stable rotational propagation condition of quantized propagation geometry.

Within this framework:

- gravity becomes rotational phase compression,
- clock-rate variation becomes propagation-rate variation,
- horizons become closure-locked propagation boundaries,
- and black-hole singularities become SI projection breakdowns beyond physically permitted propagation structure.

The Schwarzschild closure condition:

$$\frac{Gm_a}{c^2} = \lambda_C \tag{16}$$

therefore represents the propagation-boundary transition between partially free and fully trapped chronovibrational transport.

The analysis suggests that gravitational physics, quantum propagation, and electromagnetic propagation emerge from a unified rotational ledger structure rather than from independent foundational interactions.

Acknowledgments

The Quantum AetherDynamics Institute (QADI) is a private 501(c)(3) research institute developing the Aether Physics Model (APM) and Quantum Measurement Units (QMU) Thomson III [2025]. Publications and data are archived with DOIs in the AetherPhysics Zenodo community: zenodo.org/communities/aetherphysics.

References

Yakir Aharonov and David Bohm. Significance of electromagnetic potentials in the quantum theory. *Physical Review*, 115(3):485–491, 1959. doi: 10.1103/PhysRev.115.485.

Neil Ashby. Relativity in the global positioning system. *Living Reviews in Relativity*, 6(1), 2003. doi: 10.12942/lrr-2003-1.

James M. Bardeen, Brandon Carter, and Stephen W. Hawking. The four laws of black hole mechanics. *Communications in Mathematical Physics*, 31:161–170, 1973. doi: 10.1007/BF01645742.

Jacob D. Bekenstein. Black holes and entropy. *Physical Review D*, 7(8):2333–2346, 1973. doi: 10.1103/PhysRevD.7.2333.

M. V. Berry. Quantal phase factors accompanying adiabatic changes. *Proceedings of the Royal Society of London. Series A, Mathematical and Physical Sciences*, 392(1802):45–57, 1984. doi: 10.1098/rspa.1984.0023.

Albert Einstein. Die Grundlage der allgemeinen Relativitätstheorie. *Annalen der Physik*, 354(7): 769–822, 1916. doi: 10.1002/andp.19163540702.

J. C. Hafele and Richard E. Keating. Around-the-world atomic clocks: Observed relativistic time gains. *Science*, 177(4044):168–170, 1972a. doi: 10.1126/science.177.4044.168.

J. C. Hafele and Richard E. Keating. Around-the-world atomic clocks: Predicted relativistic time gains. *Science*, 177(4044):166–168, 1972b. doi: 10.1126/science.177.4044.166.

Stephen W. Hawking. Particle creation by black holes. *Communications in Mathematical Physics*, 43(3):199–220, 1975. doi: 10.1007/BF02345020.

Roy P. Kerr. Gravitational field of a spinning mass as an example of algebraically special metrics. *Physical Review Letters*, 11(5):237–238, 1963. doi: 10.1103/PhysRevLett.11.237.

R. V. Pound and G. A. Rebka. Apparent weight of photons. *Physical Review Letters*, 4(7):337–341, 1960. doi: 10.1103/PhysRevLett.4.337.

Georges Sagnac. L'ether lumineux demontre par l'effet du vent relatif d'ether dans un interferometre en rotation uniforme. *Comptes Rendus de l'Academie des Sciences*, 157:708–710, 1913.

David Thomson. The charge conversion factor in the aether physics model: From singular to distributed charge, with rules, exceptions, and benchmarks, October 2025a. URL https://doi.org/10.5281/zenodo.17451188.

David Thomson. Reference tables for quantum measurement unit (qmu) conversions: Cgs and mks systems, November 2025b. URL https://doi.org/10.5281/zenodo.17683574.

David W. Thomson III. Quantum aetherdynamics institute (qadi): Community doi overview and citation guide. Zenodo, 2025. URL https://doi.org/10.5281/zenodo.17479314.

Robert M. Wald. *General Relativity*. University of Chicago Press, Chicago, 1984. ISBN 9780226870335.